Thermal and Thermomechanical Properties of Hyperbranched Polyurethane-Urea/Cenosphere Hybrids

Kishore K. Jena, Aswini K. Mishra, K. V. S. N. Raju

Organic Coatings and Polymers Division, Indian Institute of Chemical Technology, Tarnaka, Hyderabad-500607, India

Received 22 November 2007; accepted 7 June 2008
DOI 10.1002/app.28972
Published online 23 September 2008 in Wiley InterScience (www.interscience.wiley.com).

ABSTRACT: Hyperbranched polyurethane (HBPU)-urea/cenosphere hybrid coatings were synthesized by incorporating various concentrations of cenosphere into HB polyester matrix by ultrasonication technique, and this polyester was further used for the preparation of isocyanate terminated HBPU prepolymers by reacting with excess isophorone diisocyanate (IPDI) in a NCO/OH ratio of 1.6 : 1. The desired hybrid coating is obtained by moisture curing the excess NCO present in the prepolymer through film casting. The structure of the hyperbranched polyester (HBPE) was conformed by ^{1}H, ^{13}C NMR and FTIR spectroscopy and the degree of branching (DB) was calculated using Frechet and Frey equations. These hybrid films were characterized by powder XRD, FTIR, SEM, DMTA, and TGA. The structure property correlation, intermolecular/intramolecular hydrogen bonding, the surface morphology, and viscoelastic properties were studied. These results showed an increase in T_g and thermal stability of the hybrid coatings than the base polymer. © 2008 Wiley Periodicals, Inc. J Appl Polym Sci 110: 4022–4033, 2008

Key words: hyperbranched polyols; polyurethane; cenosphere; NMR; XRD; FTIR; SEM; DMTA; TGA; T_g; thermal stability

INTRODUCTION

To deal with environmental protection agency regulations, several research efforts have been focused on developing new methodologies such as use of highly functionalized polymers like hyperbranched polymers, nanotechnology, etc. The hyperbranched polymers have been generally recognized as more economical than their counterparts because they can be synthesized easily with significantly lower manufacturing costs. The physical and chemical properties of some crosslinked hyperbranched polymer have been reported in literature.[1–9]

The organic-inorganic hybrid materials have become an increasing area of interest in today's scientific research, in view of the fact that these materials improve the thermal and mechanical properties of the polymers. These materials enhance the performance of the base polymer with the addition of small amounts of inorganic material. The literature reports the use of montmorillonite clays as fillers for nanocomposites formulation with improved properties[10–13] Particularly, more research has been devoted to develop hyperbranched polymer-clay nanocomposites, wherein, clay particles continue to be interesting filler materials for polymers in developing cost-effective high-performance coatings. Indeed, it is known from the literature that fillers such as zeolites, mica, and monomontrilonite can also improve physical and mechanical properties of the base polymers.[14–18]

Cenospheres are lightweight, inert, hollow spheres comprised largely of silica and alumina filled with gases such as air. These are naturally occurring byproducts of the burning process at coal-fired power plants, and they have some of the same properties as synthetic hollow-sphere products. Cenosphere consists of quartz and mullite as crystalline phases and some quantity of glassy phase.[19] Cenosphere have valuable applications as fillers in the manufacture of paints, plastics, ceramics, adhesives, and metal alloys. Keeping in view to the above factors, in this article cenosphere at different levels were incorporated to study the structure property correlation of hyperbranched polyester (HBPEs) and HBPU-urea/cenosphere hybrid coatings by different instrumental methods: FTIR, SEM, TGA, and DMTA.

EXPERIMENTAL

Materials

Pentaerythritol (PE), Bis-MPA, IPDI (*Z* and *E* isomer in 3 : 1 ratio) and dibutyltin dilaurate (DBTL) from Aldrich Chemicals (Milwaukee, WI); dimethyl formamide (DMF), sulfur free toluene from S.D fine chemicals (Mumbai, India). Titanium tetraisopropoxide

Correspondence to: K. V. S. N. Raju (kvsnraju@iict.res.in or drkvsnraju@gmail.com).

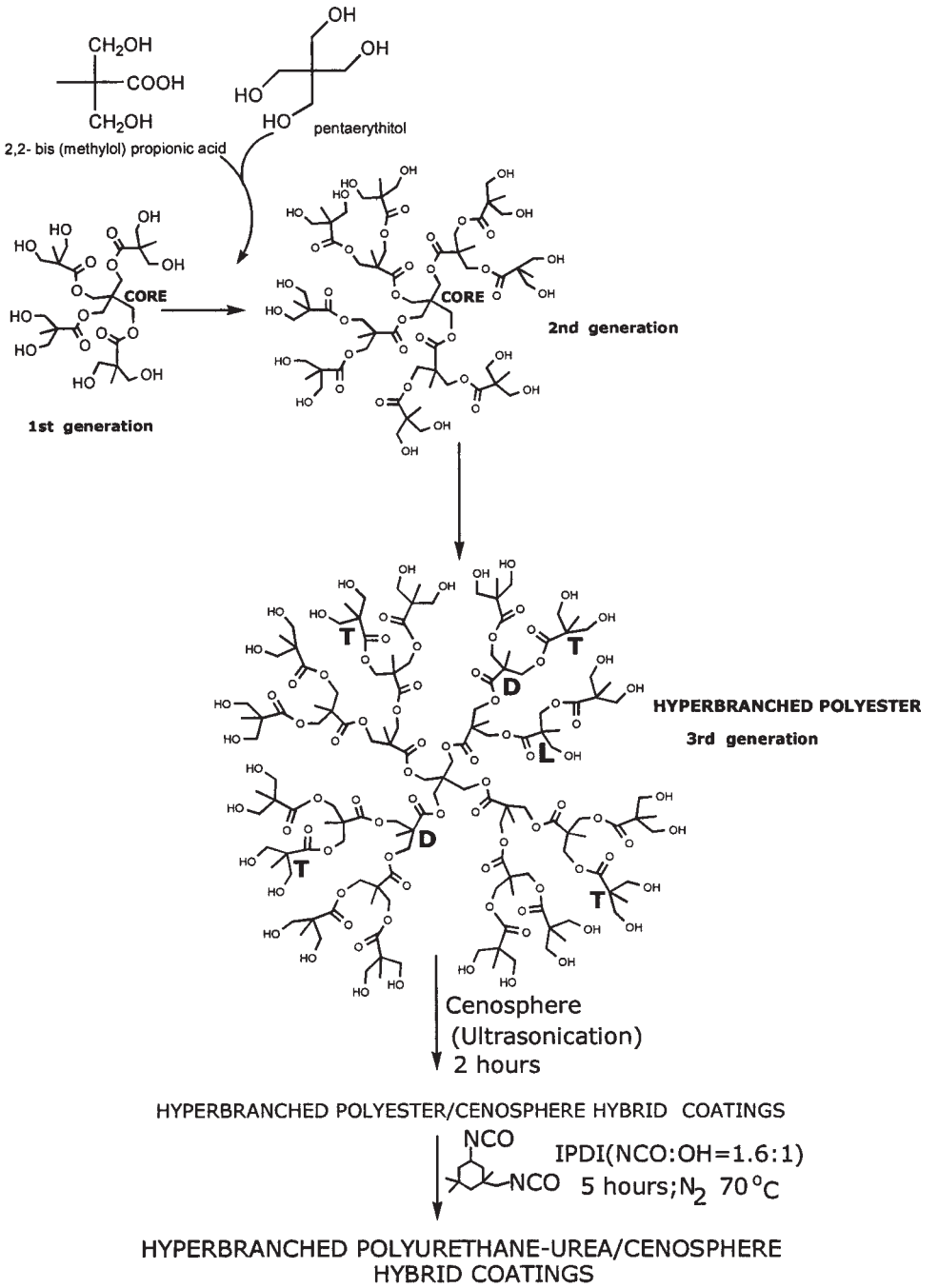

Figure 1 Synthetic scheme of HBPU-urea/Cenosphere hybrid coatings from hyperbranched polyester.

(TTIP) was purchased from Fluka Chemical Corp. (Ronkonkoma, NY) were used as received. Cenosphere was obtained from Navocrete (Hyderabad, India).

Synthesis of hyperbranched polyester polyol

Bis-MPA and PE was charged into a 500-mL round-bottom flask equipped with a mechanical stirrer, thermometer with a temperature controller, nitrogen inlet, a condenser, and a heating mantle. The esterification reaction was carried out at 170–180°C under nitrogen using 0.05 wt % TTIP. The reaction was monitored by checking the acid value and was stopped when the acid value reached below five. Similarly for the second and third generation of HBPEs (hyperbranched polyester) were prepared in a stepwise manner from the first generation polyester by adding required amount of Bis-MPA monomer. HBPE-1 was named as first generation polyester, HBPE-2 and HBPE-3 as second and third generation polyester.[20,21]

TABLE I
Different Monomer and Their Equivalent Ratio Used for the Preparation of HBPU-Urea/Cenosphere Hybrid Coatings

Polyester sample name	Chemical composition	Generation	Hybrid films sample name	NCO : OH
HBPE-1	PE + DMPA	First	$HPNG_1$ (1%)	1.6 : 1
			$HPNG_1$ (2%)	
			$HPNG_1$ (3%)	
			$HPNG_1$ (4%)	
			$HPNG_1$ (5%)	
HBPE-2		Second	$HPNG_2$ (1%)	
			$HPNG_2$ (2%)	
			$HPNG_2$ (3%)	
			$HPNG_2$ (4%)	
			$HPNG_2$ (5%)	
HBPE-3		Third	$HPNG_3$ (1%)	
			$HPNG_3$ (2%)	
			$HPNG_3$ (3%)	
			$HPNG_3$ (4%)	
			$HPNG_3$ (5%)	

Synthesis of HBPU-urea/cenosphere hybrid coatings

HBPU-urea/cenosphere hybrid coatings were prepared by dispersing required amount of cenospheres into the HBPE matrix by taking with DMF as the solvent. The dispersion of the filler into the HBPE matrix was done by using an ultrasonication technique, then the cenosphere-dispersed polyester was reacted with IPDI by a NCO/OH equivalent ratio of 1.6 : 1 for 7 h at 70–80°C in a nitrogen atmosphere. The prepared HBPU-urea/cenosphere prepolymers were coated on tin foil using manual applicator and allowed to cure at 30°C and 50% RH till the disappearance of NCO peak in FTIR spectroscopy. The prepared HBPU-urea/cenosphere hybrid samples were named as $HPNG_1$ (1%) to $HPNG_1$ (5%), $HPNG_2$ (1%) to $HPNG_2$ (5%) and $HPNG_3$ (1%) to $HPNG_3$ (5%) from first, second and third generation polyester, where G_1, G_2, and G_3 represented as first, second and third generation, respectively. The samples prepared without cenosphere were named as $HPNG_1$ (0%), $HPNG_2$ (0%), and $HPNG_3$ (0%). The preparation of HBPU-urea/cenosphere hybrid coating is shown in (Fig. 1), whereas the different reactants used to prepare the HBPU-urea/cenosphere hybrid coatings from first, second and third generation HBPEs with different wt % of cenosphere were reported in Table I.

Characterization techniques

^1H and ^{13}C NMR were used to determine the structural conformation of the synthesized hyperbranched

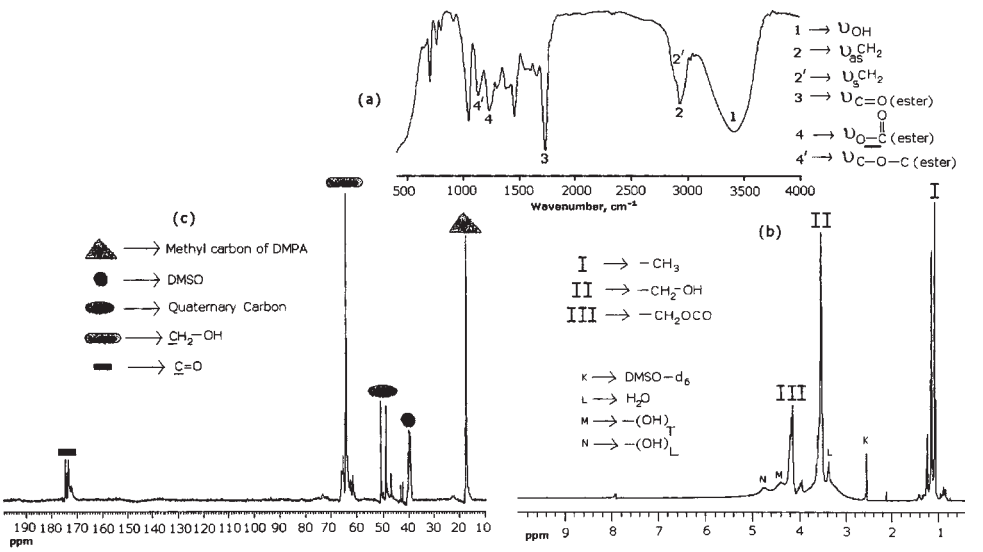

Figure 2 (a) The representative FTIR spectrum hyperbranched polyester HBPE-1, (b) ^1H NMR spectrum of HBPE-1 and (c) ^{13}C NMR spectrum of HBPE-1 recorded at room temperature.

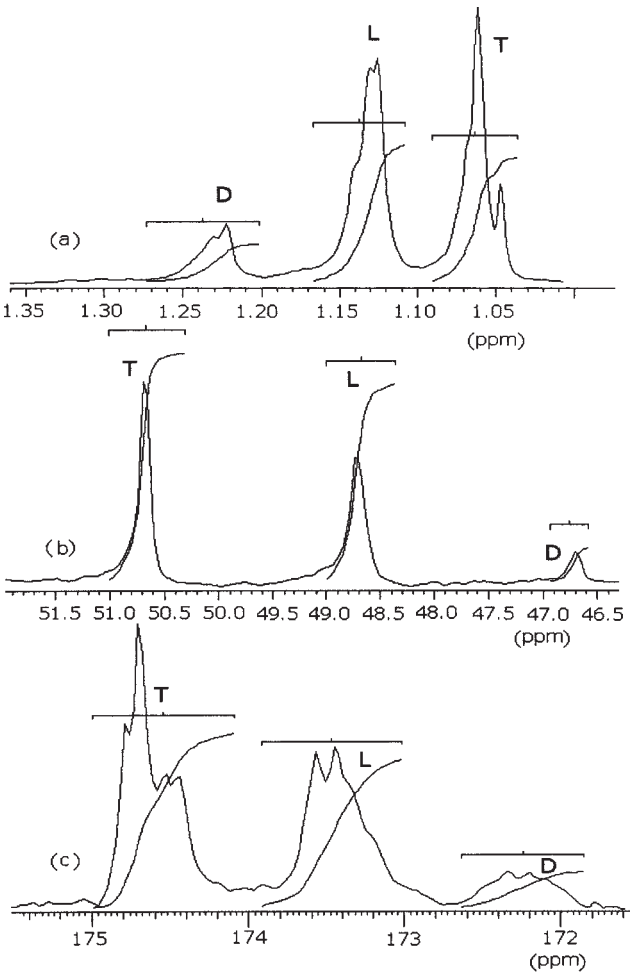

Figure 3 Determination of D, L, T from HBPE-1 by NMR, (a) $^{1}H,CH_3$; (b) ^{13}C, quaternary carbon; (c) ^{13}C, C=O.

polyesters. Nuclear magnetic resonance (^{1}H NMR and ^{13}C NMR) spectra were recorded with a Varian VXR-Unity 200 MHz and Bruker UXNMR 300 MHz spectrometer in room temperature, using DMSO-d_6 as a solvent and δ values relative to Me_4Si (TMS). Zeta particle size analyzer, Malvern Instruments (Malvern, UK) has been employed to study the particle size distribution of the sample. XRD pattern for the cenosphere, hyperbranched polymer and hybrid samples were attained using a Siemens/D-5000 X-ray diffractometer using Cu Kα radiation of wavelength 1.54 Å. Morphology of hybrid sample was found out using Hitachi S520 scanning electron microscope instrument operating at 10 kV. The FTIR spectra of the KBr coated samples were scanned on a Thermo Nicolet Nexus 670 spectrometer with resolution of 4 cm^{-1} and in the range of 400–4000 cm^{-1}. To identify the complex bands in the N—H and C=O zone, the curve-fitting simulations were performed using Origin 6.0 software. The DMTA IV scan (Rheometric Scientific, USA) was performed in tensile mode in the temperature range from 30 to 250°C with a heating rate of 3°C/min using sample of 15 × 10 × 0.15 mm^3 at a frequency of 1 Hz. The E' values in rubbery region at $T > T_g$ are taken to calculate crosslink density, υe by using the following equation:

$$\upsilon e = E'/3RT \quad (1)$$

where, R is universal gas constant and T is temperature and distance between two crosslinks, M_c was calculated by using following equation:

$$M_c = \rho/\upsilon e \quad (2)$$

where, ρ is the density of the film.[22,23] TGA of the hybrid samples has been conducted by using thermal analyzer (Perkin ElmerTGA-7, Shimadzu, Japan) with 10–15 mg of the sample at the heating rate of 10°C/min in N_2 atmosphere from 30 to 600°C.

RESULTS AND DISCUSSION

NMR analysis

The ^{1}H NMR spectrum of HBPE-1 at room temperature is shown in Figure 2(b). The —CH_3 protons in terminal, linear, and dendritic divisions resonate at: δ ppm; 1.02, 1.07, and 1.17, respectively.[20,24] The unreacted carboxyl groups of Bis-MPA resonate at: δ ppm; 12–13 but from the Figure 2(b), it was confirmed that the unreacted carboxyl group in the polyester was absent. The —CH_2 groups attached to the reacted —$COOCH_2$ and unreacted —CH_2OH groups resonate at: δ ppm; 4.2 and 3.5. The chemical shift of —CH_2OH coincides with H_2O (δ 3.3 ppm) protons

TABLE II
^{1}H and ^{13}C-NMR Analysis of Hyperbranched Polyester (HBPE)

Sample name	Chemical shift values	[D]	[L]	[T]	DB_{rechet}	DB_{Frey}
HBPE-1	CH_3 (^{1}H, 1.0–1.35 ppm)	0.131	0.469	0.40	53.1	35.8
	C_q (^{13}C, 46.5–51.5 ppm)	0.11	0.46	0.43	54.0	32.0
	C=O (^{13}C, 171.5–175 ppm	0.10	0.40	0.50	60.0	33.3
HBPE-2	CH_3 (^{1}H, 0.9–1.37 ppm)	0.128	0.492	0.38	50.8	34.22
HBPE-3	CH_3 (^{1}H, 1.1–1.39 ppm)	0.10	0.51	0.39	49.0	28.16

D, Dendritic; L, Linear; T, Terminal; C_q, quaternary carbon zone; DB, degree of branching.

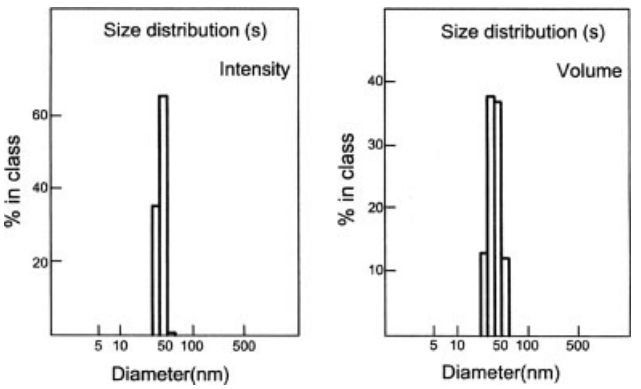

Figure 4 Particle size distribution characteristics for the cenosphere sample.

because the sample was carried out in room temperature. The ^{13}C NMR spectrum of sample HBPE-1 at room temperature is shown in Figure 2(c). The methyl groups of Bis-MPA, quaternary carbons (C_q), methylene groups and carbonyl groups resonate at: δ ppm; 17, 45–51, 62–68, and 171–175. Dendritic unit (*D*), linear unit (*L*) and terminal unit (*T*) can be distinguished both by ^1H NMR using the $-CH_3$ zone and by ^{13}C NMR using both C=O and quaternary carbon (C_q). These particular areas of the NMR spectra of HBPE-1 are presented in Figure 3. The degree of branching (DB) of the HBPE-1, HBPE-2 and HBPE-3 samples were calculated by using Frechet or Frey equations[25,26] and are reported in Table II.

$$\text{By Frechet}: \ \mathrm{DB}_{\mathrm{Frechet}}[D + T/D + L + T] \quad (3)$$

$$\text{Frey}: \ \mathrm{DB}_{\mathrm{Frey}} = [2D/2D + L] \quad (4)$$

Particle size distribution

Figure 4 presents particle size distribution of the cenosphere sample using a laser particle size analyzer. From Figure 4, it can be noticed that the cenosphere sample consists of particles (in majority) with diameter ranging from 28 to 55 nm. However, few particles with maximum diameter of 45 nm were also noticed in the sample.

XRD analysis

The predominant broad peak is attributed at about $2\theta = 17.5°$ is shown in Figure 5(a), which may be the base peak of HBPU-urea. XRD analysis of pure cenosphere particle is shown in [Fig. 5(b)], however, all sharp peaks were corresponds to the major

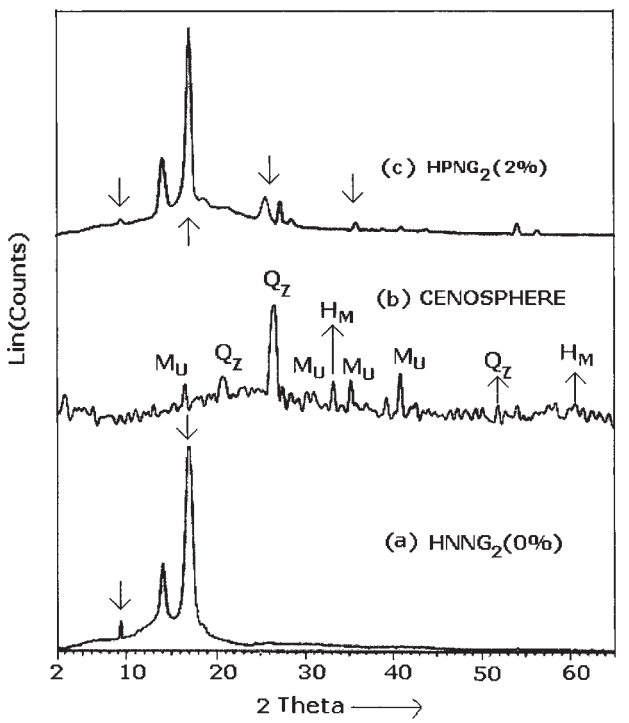

Figure 5 A comparison of X-ray diffraction spectra of (a) $HPNG_2$ (0%); (b) Pure cenosphere; Q_Z: quartz, M_U: mullite, H_M: hematite (c) hybrid coatings of $HPNG_2$ with 2 wt % cenosphere.

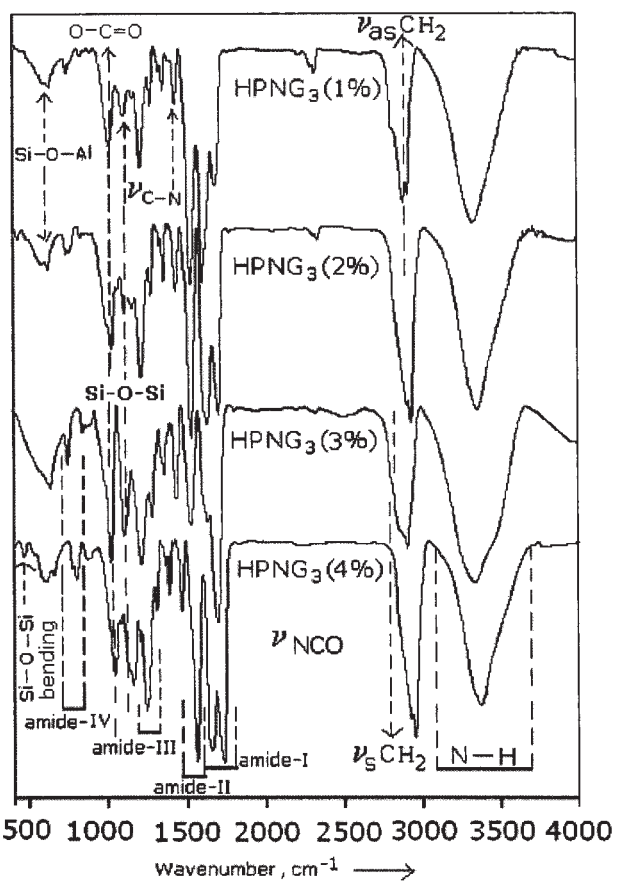

Figure 6 The full FTIR spectra of HBPU-urea/cenosphere hybrid thin films in the zone 400–4000 cm^{-1} (NCO: OH=1.6 : 1) with cenosphere percentage recorded at room temperature.

TABLE III
The Characteristic FTIR Bands, of the HBPU-Urea/ Cenosphere Hybrid Coatings

3050–3750 cm^{-1}	N—H stretching vibrations
2800–3000 cm^{-1}	C—H stretching vibrations
2957 cm^{-1}	Asymmetric —CH_3 stretching
2872 cm^{-1}	Symmetric —CH_3 stretching
2920 cm^{-1}	Asymmetric —CH_2 stretching
2851 cm^{-1}	Symmetric —CH_2 stretching
1600–1800 cm^{-1}	Amide I, —C=O stretching vibrations
1500– 1589 cm^{-1}	Amide II, C—N stretching (ν_{C-N}) and N_H bending (δ_{N-H})
1200–1292 cm^{-1}	Amide III,$\delta_{N-H} + \nu_{C-N}$
1067 cm^{-1}	O—C=O stretching in hard urethane segment and esteric C—O stretching vibrations
1190 cm^{-1}	(ν—COC—) from the esters of HBPEs
1002–1012 cm^{-1}	Stretching and rocking vibrations of the C—C and —CH_2 groups
767 cm^{-1}	Amide IV
658 cm^{-1}	Amide V

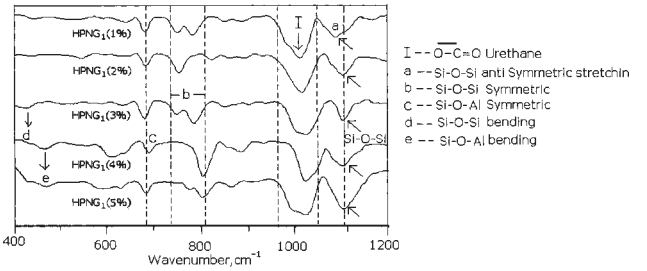

Figure 7 FTIR spectra of first generation (G_1) in the zone 400–1200 cm^{-1} with different cenosphere percentage.

phases: quartz, mullite (aluminum silicate) and iron oxide (hematite) and was noticed some quantity of amorphous phase.[19] It was observed that the peak intensity of quartz (Q_Z) in the pure cenosphere is much greater. The thicknesses of the crystallites comprising the cenosphere were estimated to be 22–50 nm by Scherrer's equation and were similar to values obtained from particle size distribution analysis. The XRD pattern for $HPNG_2$ (2%) hybrid is shown in Figure 5(c). Addition of cenospheres modified the intensities of base polymer peaks present in the hybrid composite. The intensity of the HBPU-urea peak decreases on hybrid composite, which may be due to increase in the discontinuity of the base polymer structure.[27] The HBPU-urea/cenosphere hybrid shows the additional peaks at 2θ = 25.5, 34.0, 35.5, 37.0, 41.0, and 54.5° that correspond to the major reflections of quartz, iron oxide (hematite) and mullite (aluminum silicate), respectively, of cenosphere structure.[19,27]

FTIR analysis

The FTIR spectrum of the HBPE-1 in the zone 400–4000cm^{-1} is illustrated in Figure 2(a). The broad peak at 3425 cm^{-1} is attributed to the O—H stretching absorbance and the C=O strong band at 1754 cm^{-1} comes from the ester linkages. The broad complex band of the hydroxyl (δ O—H) vibration region at about 3425 cm^{-1} is attributed to the combined effect of the differently associated hydroxyl groups, i.e., hydrogen bonding between —OH and —OH or between —OH and —C=O group of more electronegative ester function.[20,28,29] Few reports are

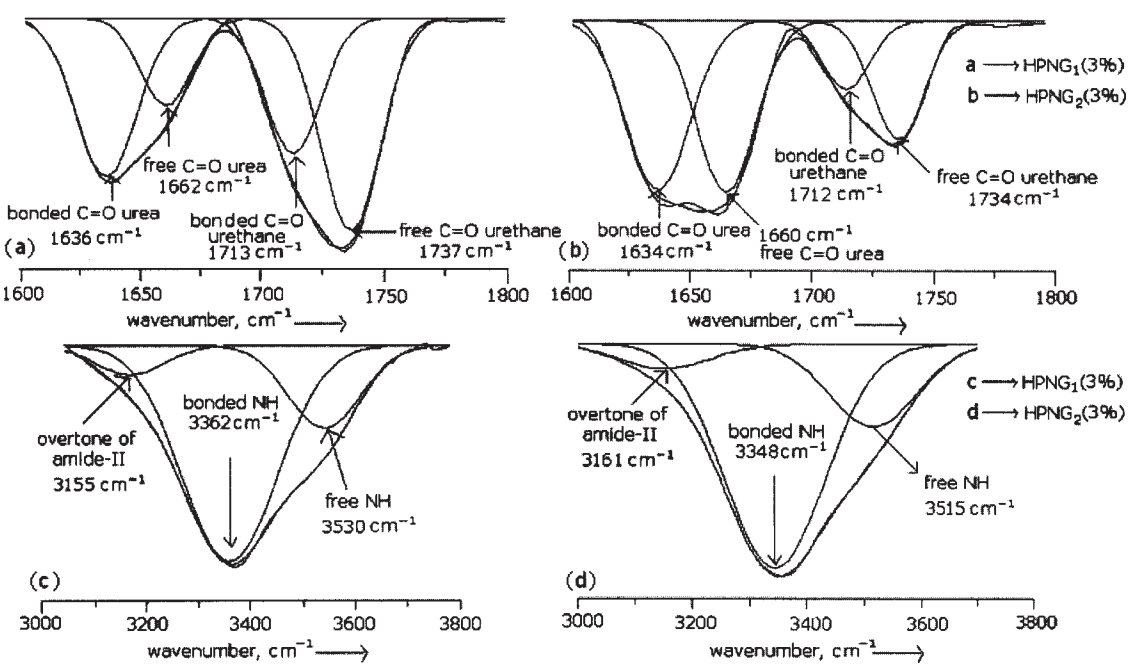

Figure 8 Deconvoluted C=O zone and N(H zone of $HPNG_1$ (3%) and $HPNG_2$ (3%) hybrid coatings.

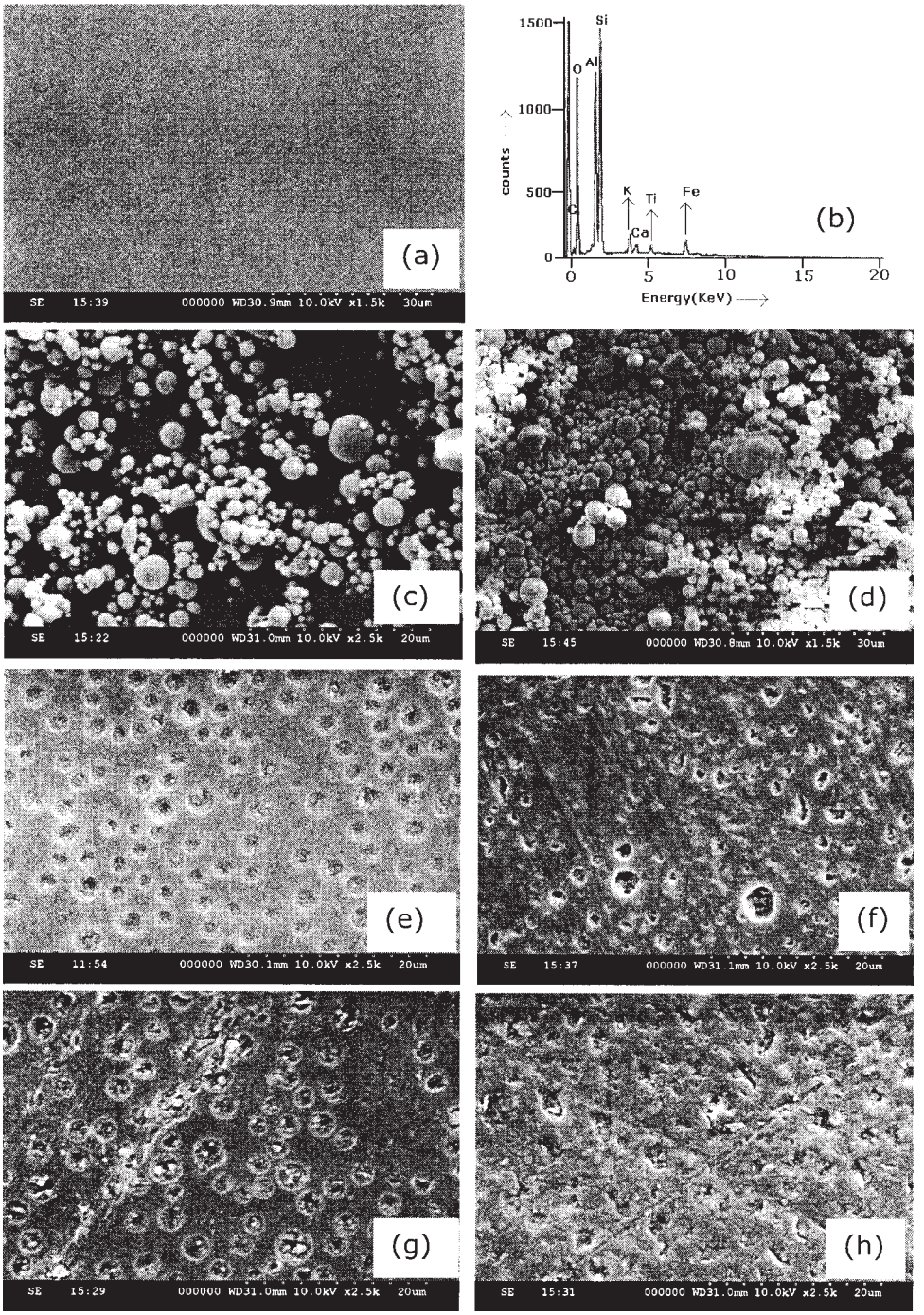

Figure 9 SEM/EDAX results of HBPU-urea/cenosphere hybrid coatings: (a) $HPNG_2$ (0%); (b) EDAX cenosphere; (c) and (d) pure cenosphere; (e)–(h) $HPNG_2$ (2%)–(5%).

available on the study of hydrogen bonding interaction in polyurethane coatings.[29–32] Figure 6 illustrates the FTIR spectra of HBPU-urea/cenosphere hybrid coatings in the zone 400–4000 cm^{-1}. The characteristic bands of the HBPU-urea/cenosphere hybrid samples were given in Table III.[33–37]

The representative FTIR spectra of $HPNG_1$ (1%) to $HPNG_1$ (5%) films in the zone 400–1200 cm^{-1} are shown in Figure 7. Cenosphere containing HBPE exhibits new absorption peaks distinctly at 1090 cm^{-1} which are assigned to the antisymmetric stretching vibration of Si—O—Si and the band at 790–810 cm^{-1} corresponding to the symmetric vibration. The band at 1130–1170 cm^{-1} is assigned to the antisymmetric stretching vibration of Si—O—Al and the band at 700 cm^{-1} to the symmetric Si—O—Al

TABLE IV
Element (%) of the Cenosphere and Hybrid Samples on EDAX

Sample code	Elements	Percentage	TGA Residue at 600°C
Cenosphere	O	57.01	
	Al	14.57	
	Si	21.23	
	K	0.93	
	Ca	0.78	
	Ti	1.24	
	Fe	4.24	
$HPNG_2$ (2%)	Si	1.21	5.31
$HPNG_2$ (3%)		2.36	11.52
$HPNG_2$ (4%)		3.14	15.81

stretching vibration.[21] The band at 470 cm^{-1} is assigned to the O—Si—O bending vibration, which is due to the presence of various metal oxides in the hybrid. There was not much variation in the characteristic peaks of FTIR spectra of these samples. To recognize the structural effect variables on the hydrogen bonding of these samples, the deconvolution of N—H (3000–3800 cm^{-1}) and C=O (1600–1800 cm^{-1}) stretching zone was done. This is to simplify of complex spectra consisting of many overlapped peaks.

The C=O stretching zone

The C=O region of the FTIR spectra provides important information in understanding the extent of hydrogen bonding in these HBPU-urea/cenosphere hybrid coatings. The C=O peak deconvolution of $HPNG_1$ (3%) and $HPNG_2$ (3%) coatings are shown in Figures 8(a, b). The bands assigned to the urethane group are centered at ~ 1732–1738 cm^{-1} (free C=O from urethane) and 1710–1714 cm^{-1} (bonded C=O from urethane groups), respectively. The bands assigned to the free and bonded groups centered at ~ 1660–1663 cm^{-1} (free C=O urea groups) and at 1630–1637 cm^{-1} (bonded C=O from urea groups), respectively.[38,32,21]

The N—H stretching zone

The representative deconvoluted spectra of $HPNG_1$ (3%) and $HPNG_2$ (3%) are shown in Figure 8(c,d). The bands are centered at ~ 3515–3530 cm^{-1} (free N—H groups), 3345–3365 cm^{-1} (bonded N—H groups). An overtone of amide-II causes deformation vibration of N—H group increased by Fermi resonance centered at 3155–3162 cm^{-1}.[39]

SEM analysis

The SEM micrograph of $HPNG_2$ (0%) is shown Figure 9(a) and it is clear that the sample is homogeneous in nature.[19] Typical SEM micrographs of cenosphere are shown in Figure 9(c,d). Cenosphere is overall more spherical in shape and but shows a large variation in their size. Typical EDAX spectrum showing the microchemistry of the cenosphere particles is also shown in Figure 9(b). The main elements detected by EDAX of this cenosphere were aluminum, silicon, oxygen, and small quantities of K, Ca, Fe, Ti, and C. Table IV shows the element composition of the cenosphere and hybrid from EDAX. SEM micrographs of $HPNG_2$ (2%), $HPNG_2$ (3%), $HPNG_2$ (4%), and $HPNG_2$ (5%) hybrid coatings are shown in Figure 9(e–h). These micrographs were observed that the presence of spherical cenosphere particles in HBPU-urea, which are homogeneously embedded.

Contact angle measurement

In the present study, the hydrophilicity and hydrophobic nature of the samples with different weight percentage of cenosphere content were evaluated by measuring the contact angle formed between water drop and the surface of the samples using contact angle measuring system G 10 (KRUSS). The results obtained are reported in Table V. It can be confirmed that the improvement of the hydrophobic capacity of HBPU-urea/cenosphere hybrid coatings. In fact, the polar component decreases with the addition of cenosphere. These coatings have been made on HBPU-urea. The formulation, without cenosphere, leads to a water contact angle of 57.5°. With HBPU-urea/cenosphere coating, the contact angle increases by at least 8–9°. Table V shows that, the higher contact angle observed for the formulation $HPNG_2$ (5%) among all hybrids.

DMTA analysis

The mechanical response of the samples is measured as a function of temperature using DMTA, which provides information regarding the actual changes

TABLE V
Contact Angle of HBPU-Urea/Cenosphere Hybrid Coatings with Different Cenosphere Concentration

Sample Name	Cenosphere Wt %	Contact angle in degree (After 15 days curing)
$HPNG_2$	0	57.5
	1	65.1
	2	73.2
	3	80.6
	4	84.2
	5	93.6
$HPNG_1$	5	91.8
$HPNG_2$	5	93.6
$HPNG_3$	5	92.1

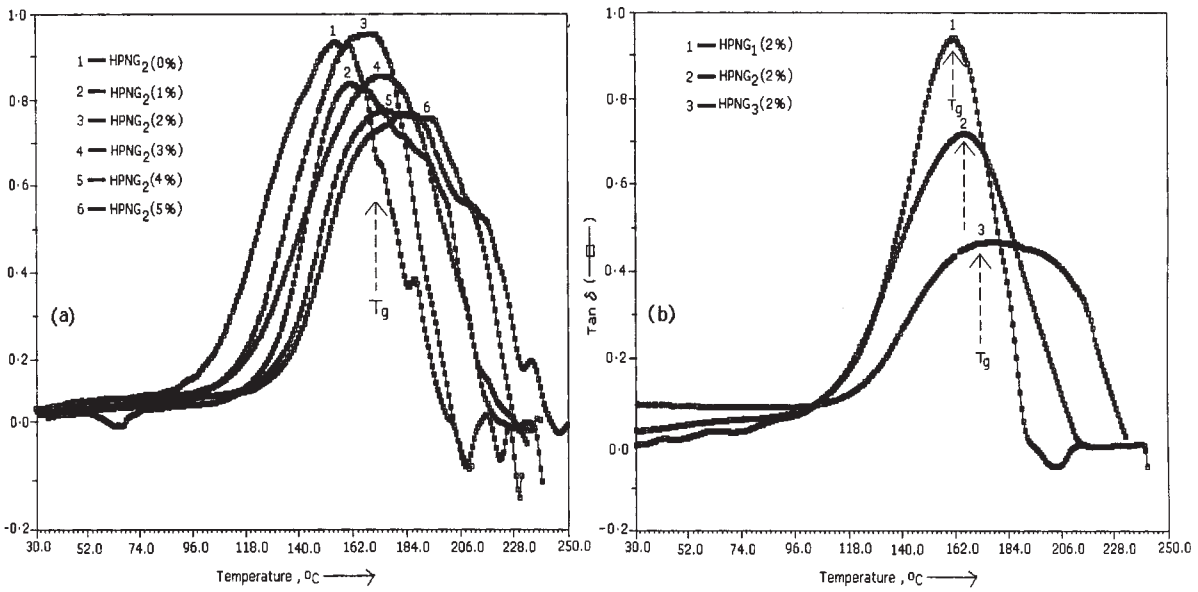

Figure 10 DMTA results of HBPU-urea/cenosphere hybrid coatings: (a) tan δ versus temperature of $HPNG_2$ (0%) to $HPNG_2$ (5%) hybrid coatings; (b) tan δ versus temperature of $HPNG_1$ (2%), $HPNG_2$ (2%), and $HPNG_3$ (2%) hybrid coatings.

in viscoelastic properties of hybrids when exposed to elevated temperatures. The DMTA results were used to analyze the glass transition temperature (T_g) and the storage modulus (E') of HBPU-urea/cenosphere hybrid coatings prepared from various generations HBPE containing 1–5 wt % cenosphere. Figure 10(a) shows the tan δ versus temperature spectra of $HPNG_2$ (0%) to $HPNG_2$ (5%) coating films at a heating rate of 3°C/min and 1 Hz test frequency. The T_g values of with and without cenosphere samples [shown in Figure 10(a).] were listed in Table VI. On comparison of the above spectra, the T_g value of $HPNG_2$ (0%) was less than that of samples containing cenosphere and increases with increasing the cenosphere content in the coatings. The rise in the T_g may be attributed to loss of mobility of the polymer chains located near the solid cenosphere surfaces. The T_g values between $HPNG_2$ (0%), $HPNG_2$ (1%), $HPNG_2$ (2%), $HPNG_2$ (3%), $HPNG_2$ (4%), and $HPNG_2$ (5%) were in the following order: $HPNG_2$ (5%) > $HPNG_2$ (4%) > $HPNG_2$ (3%) > $HPNG_2$ (2%) > $HPNG_2$ (1%) > $HPNG_2$ (0%). The phenomenon may be due to inclusion of these particles shows good interfacial bonding such as, hydrogen bonding between filler surface and functional groups of polymers. This arrangement of polymer chains affects the interfacial mechanical properties, which restricts the free movement of the polymer matrix around it and hence increases overall coating stiffness and T_g.[27] The tan δ versus temperature spectra of $HPNG_1$ (2%), $HPNG_2$ (2%) and $HPNG_3$ (2%) coating films were presented in Figure 10(b). The values of T_g, E', υe, M_c, and T_s of the hybrid cenosphere films were reported in Table VI. For the calculation of υe, M_c, the E' values were taken at T_g + 5°C in the DMTA spectra. The E' (T_g + 5°C) values of the hybrid coatings with respect to filler effect are shown in Figure 11. The hybrid coatings showed increased storage modulus (E'), which could be due to the hydrogen bonding interaction between cenosphere and polymeric chains. The observed E' peaks (figure not shown) were shifted to higher temperature with increasing cenosphere percent. There are no significant difference in E'' at 40°C of the hybrid coatings but decreased above T_g.[40,41] The values of crosslink density indicate that $HPNG_3$ (2%) hybrid coatings were closely packed network as compared to $HPNG_1$ (2%), $HPNG_2$ (2%).

TABLE VI
DMTA Data of Different HBPU-Urea/Cenosphere Hybrid Coatings

				$HPNG_2$					
Sample code	$HPNG_1$ (2%)	$HPNG_2$ (2%)	$HPNG_3$ (2%)	0%	1%	2%	3%	4%	5%
E', [Pa], at T_g+5 °C)	1.97×10^7	3.09×10^7	1.86×10^8	2.47×10^7	2.81×10^7	3.09×10^7	3.89×10^7	1.88×10^8	1.92×10^8
T_g °K	432.44	439.92	447.81	429.12	435.13	439.92	448.18	452.32	459.44
T_s °K	388.18	392.95	398.95	380.67	383.22	392.95	393.38	393.98	400.20
T_s/T_g	0.897	0.895	0.890	0.874	0.880	0.895	0.877	0.871	0.870
υe, mol/cm^3 $\times 10^3$	1.80	2.78	16.41	2.28	2.55	2.78	3.44	16.48	25.89
M_c, g/mol $\rho = 1.11$	613.25	399.28	67.68	486.84	435.29	399.28	322.67	67.35	42.87

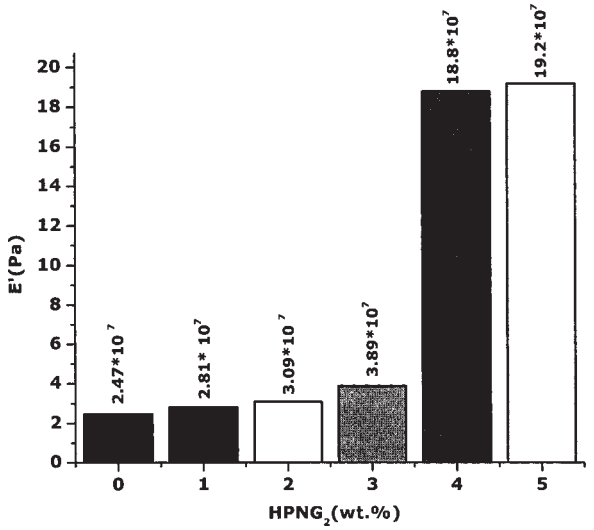

Figure 11 The E' (at T_g + 5°C) variation with increasing the cenosphere content.

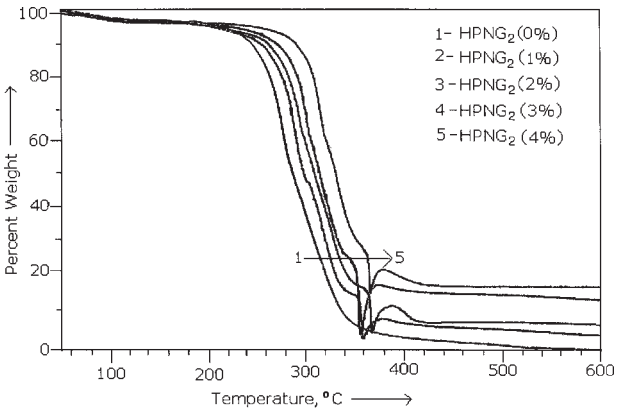

Figure 12 The TGA spectra of different HBPU-urea/cenosphere hybrid coatings, with increasing the cenosphere content.

Generally, the higher the crosslink density lowers the elastically effective chain length (M_c) and the film was harder.[42–44] Thus, the coating $HPNG_3$ (2%) was harder than their counter parts. Comparison of T_g values $HPNG_1$ (2%), $HPNG_2$ (2%), and $HPNG_3$ (2%) were observed that the third generation hybrid film T_g value is more as compared to first and second generation. This indicates that the T_g increases with increasing the generation number of hyperbranched polyester. The T_s/T_g ratio expresses the width of the tan δ peak, which suggests that higher T_s/T_g ratio leads to a narrow tan δ peak.[45,46] This was confirmed by the observed values of T_s/T_g, which were reported in Table VI. The peak width was found to be narrow for first and second generation and broad for third generation system, which point toward that crosslink density maximum for third generation system. It may be due to the hindered cooperative motion of the polymer chains, which shows the samples with higher crosslink density.[47–49]

TGA analysis

TGA is used to measure a variety of polymeric phenomenon involving weight changes, sorption of gases, desorption of contaminant, and degradation. Figure 12 shows the TGA thermograms for $HPNG_2$ (0%) and the corresponding hybrid coatings, obtained at a heating rate of 10°C/min, in N_2 environment. It was noticed from the TGA profile that, the thermal stability of the different hybrid coatings is higher than the base polymer. The onset degradation temperature for hybrid coatings along with 0% cenosphere was listed in Table VII, and the data shows that the onset degradation temperature shifts to higher temperature side on increasing the cenosphere content. This improvement in thermal stability may be due to the interlocking of cenosphere functional groups and polymeric chains that present on the surface and inside the film by hydrogen bonding.[50,51] The formation of hydrogen bonding in the hybrid coatings was analyzed in the "FTIR analysis" Section. The figure also suggests that all the polymers were stable up to temperature of 260°C and the major degradation takes place above temperature of 270°C. In all the hybrid samples, small weight loss occurs up to 250°C, and this might be due to the expulsion of air or other gases physically entrapped on the surface of the hybrid coatings and cenosphere, while significant weight losses occur between a temperature ranges of 270–450°C.[52–54] For instance at 250°C, the percentage weight loss of $HPNG_2$ (0%) is 13.20% and those of the hybrids with cenosphere content 1–4% are: 8.98, 7.31, 5.28, and 3.84%, respectively. These above weight losses might be attributed due to the thermal decomposition of volatile species, water, unreacted monomer and polymer components,

TABLE VII
The Characteristic Thermal Decomposition Data of Different HBPU-Urea/Cenosphere Hybrid Coatings

Sample code	T_{on} in °C	%Weight loss at 250°C	%Weight loss at 450°C	%Residual mass at 600°C
$HPNG_2$ (0%)	260.12	13.20	98.57	0.02
$HPNG_2$ (1%)	268.91	8.98	94.22	2.47
$HPNG_2$ (2%)	273.68	7.31	93.02	5.31
$HPNG_2$ (3%)	280.12	5.28	86.13	11.52
$HPNG_2$ (4%)	295.32	3.84	82.96	15.81

present in the base polymer and hybrid coatings. In addition to this, in the temperature range of 350–400°C, the hybrid coatings exhibits a relatively small weight loses about 8%, which may be due to the complete burning off carbon in the cenosphere.[55] The percent weight loss at 450°C, of the hybrid cotings $HPNG_2$ (1%) to $HPNG_2$ (4%), and $HPNG_2$ (0%) were 94.22, 93.02, 86.13, 82.96, and 98.57%, respectively. Table VII shows the residual mass present in the hybrid coatings at 600°C.

CONCLUSIONS

Hybrid composite materials based on hyperbranched polyurethane containing different weight percentages of cenosphere were produced and their thermo mechanical properties were investigated. Detailed characterizations of hyperbranched polyurethane-urea/cenosphere hybrid composites were carried out by using NMR, XRD, FTIR, SEM, DMTA, and TGA techniques. It was observed from XRD analysis that the HBPU-urea/cenosphere hybrid composites are semicrystalline in nature. To better understand the relative influences of hydrogen bonding on the structure to property relationship, we have deconvoluted the N—H and C=O bands. The amount of hydrogen bonding and free urethane/urea groups depends on the chemical structure of the hyperbranched polyester, its generation number as well as monomers used for the preparation of hyperbranched polyols. The high silica percentage is present excess in high percentage cenosphere as compared to other in the hybrid composites was confirmed by FTIR studies. The SEM image of HBPU-urea/cenosphere hybrid composites clearly shows the presence of cenosphere and observed that the cenosphere was homogeneously distributed in all samples. Addition of cenosphere as fillers into a polymer matrix creates internal cenosphere-polymer interfaces. The damping peak (tan δ) increases and the damping curve becomes broader with increasing the cenosphere content. The storage modulus (E') of the composite films became higher with the increment of cenosphere in the analyzed range of temperature and this is more pronounced in the glassy region. Thermogravimetric results have shown that, the cenosphere content has a major influence on thermal stability of the base polymer. Therefore, it can be concluded that, the cenosphere is effective filler, for increasing properties like thermal stability and glass transition temperature.

References

1. Tomalia, D. A.; Frechet, J. M. J. J Polym Sci Part A Polym Chem 2002, 40, 2719.
2. Stiriba, S. E.; Frey, H.; Haag, R. Angew Chem 2002, 41, 1329.
3. Frechet, J. M. J. Science 1994, 263, 1710.
4. Froehling, P. E. Dyes Pigments 2001, 48, 187.
5. Vogtle, F.; Gestermann, S.; Hesse, R.; Schwierz, H.; Windisch, B. Prog Polym Sci 2000, 25, 987.
6. Frey, H.; Schlenk, C. Top Curr Chem 2000, 210, 69.
7. Roovers, J.; Comanita, B. Adv Polym Sci 1999, 142, 179.
8. Schluter, A. D.; Rabe, J. P. Angew Chem 2000, 39, 864.
9. Vukovic, J.; Steinmeier, D.; Lechner, M. D.; Jovanovic, S.; Bozic, B. Polym Degrad Stab 2006, 91, 1903.
10. Nasar, A. S.; Jikei, M.; Kakimoto, M. Eur Polym J 2003, 39, 1201.
11. Yano, K.; Usuki, A.; Okada, A.; Kurauchi, T.; Kamigaito, O. J Polym Sci Part A Polym Chem 1993, 31, 2493.
12. Yano, K.; Usuki, A.; Kada, A. J Polym Sci Part A Polym Chem 1997, 35, 2289.
13. Christopher, J. G. P.; Garamszegi, L. S.; Leterrier, Y.; Rodlert, M.; Jan-Anders, E. M. Chem Mater 2002, 14, 486.
14. Mecking, S.; Thomannn, R.; Frey, H.; Sunder, A. Macromolecules 2000, 33, 3958.
15. Schlotterbeck, U.; Aymonyier, C.; Thomann, R.; Hofmeister, H.; Tromp, M.; Richtering, W.; Mecking, S. Adv Funct Mater 2004, 14, 999.
16. Cyril, A.; Ulf, S.; Lydie, A.; Philipp, Z.; Ralf, T.; Joerg, C.T.; Stefan, M. Chem Commun 2002, 18.
17. Chau, H. H.; Jan, T.; Christina, S.; Ralf, T.; Joerg, C. T. Adv Mater 2004, 16, 957.
18. Monticelli, O.; Chincar, A.; Bianchini, C.; Vizza, F.; Moneti, S.; Russo, S. Macromolecules 2003, 36, 4294.
19. Matsunaga, T.; Kim, J. K.; Hardcastle, S.; Rohatgi, P. K. Mater Sci Eng 2002, A325, 333.
20. Jena, K. K.; Raju, K. V. S. N.; Prathab, B.; Aminabhavi, T. M. J Phys Chem B 2007, B111, 8801.
21. Jena, K. K.; Raju, K. V. S. N. Ind Eng Chem Res 2007, 46, 6408.
22. Hill, L. W. J Coating Tech 1992, 64, 29.
23. Hill, L. W. Prog Org Coat 1997, 31, 235.
24. Malmstome, E.; Hult, A. Macromolecules 1995, 28, 47.
25. Wooley, K. L.; Frechet, J. M.; Hawker, C. J Polym 1994, 35, 4489.
26. Thomasson, D.; Boisson, F.; Girard-Reydet, E.; Mechin, F. React Funct Polym 2006, 66, 1462.
27. Chand, N.; Vashishtha, S. R. Bull Mater Sci 2000, 23, 103.
28. Ubale, V. P.; Sagar, A. D.; Birajdar, M. V. J Appl Polym Sci 2001, 79, 566.
29. Yang, B.; Huang, W. M.; Li, C.; Li, L. Polymer 2006, 47, 1348.
30. Kaushiva, B. D.; Wilkes, G. L. Polymer 2000, 41, 285.
31. Schuur, M. V.; Noordover, B.; Gaymans, R. J. Polymer 2006, 47, 1091.
32. Yilgor, I.; Yilgor, E.; Guler, I. G.; Ward, T. C.; Wilkes, G. L. Polymer 2006, 47, 4105.
33. Seymour, R. W.; Estes, G. M.; Cooper, S. L. Macromolecules 1970, 3, 579.
34. Coleman, M. M.; Lee, K. H.; Skrovanek, D. J.; Painter, P. C. Macromolecules 1986, 19, 2149.
35. Wilhelm, C.; Gardette, J. L. Polymer 1998, 39, 5973.
36. Mido, Y. Spectrochim Acta 1972, 28A, 1503.
37. Chattopadhyay, D. K.; Prasad, P. S. R.; Sreedhar, B.; Raju, K. V. S. N. Prog Org Coat 2005, 54, 296.
38. Chattopadhyay, D. K.; Mishra, A. K.; Sreedhar, B.; Raju, K. V. S. N. Polym Degrad Stab 2006, 91, 1837.
39. Lee, H. S.; Wang, Y. K.; Romanova, V.; Begishev, V.; Karmanov, V.; Kondyurin, A.; Maitz, M. F. J Raman Spectrosc 2002, 33, 769.
40. Sivaraman, P.; Manoj, N. R.; Barman, S.; Chandrasekhar, L.; Mishra, V. S.; Samui, A. B.; Chakraborty, B. C. Polym Test 2004, 23, 645.
41. Fisher, I.; Zoldan, J.; Siegmann, A.; Nrkis, M. Polym Compos 2002, 23, 464.
42. Narayan, R.; Raju, K. V. S. N. Prog Org Coats 2002, 45, 59.

43. Chattopadhyay, D. K.; Panda, S. S.; Raju, K. V. S. N. Prog Org Coats 2005, 54, 10.
44. Narayan, R.; Chattopadhyay, D. K.; Sreedhar, B.; Raju, K. V. S. N. J Mater Sci 2002, 37, 4911.45.
45. Gillham, J. K. Polym Eng Sci 1986, 26, 1429.
46. Chiou, B. S.; Scheon, P. E. J Appl Polym Sci 2002, 83, 212.
47. Asif, A.; Shi, W.; Shen, X.; Nie, K. Polymer 2005, 46, 11066.
48. Zhu, P. W.; Zheng, S.; Simon, G. Macromol Chem Phys 2001, 202, 3008.
49. Chattopadhyay, D. K.; Sreedhar, B.; Raju, K. V. S. N. Polymer 2006, 47, 3814.
50. Jia, Q. M.; Zheng, M.; Zhu, Y. C.; Li, J. B.; Xu, C. Z. Eur Polym J 2007, 43, 35.
51. Prabhakarana, K.; Warriera, K. G. K.; Rohatgi, P. K. Ceram Int 2001, 27, 749.
52. Pielichowski, K. Solid State Ion 1997, 104, 123.
53. Matveeva, E. S.; Calleja, R. D.; Parkhutik, V. P. Synth Met 1995, 72, 105.
54. Han, M. G.; Lee, Y. J.; Byun, S. W.; Im, S. S. Synth Met 2001, 124, 337.
55. Arenillas, A.; Smith, K. M.; Drage, T. C.; Snape, C. E. Fuel 2005, 84, 2204.